INTERNATIONAL JOURNAL OF UROLOGY
International Journal of Urology (2020) doi: 10.1111/iju.14238

Original Article

Novel implantable pressure and acceleration sensor for bladder monitoring

Mohammad Ayodhia Soebadi,[1,2,3,4] Tristan Weydts,[5] Luigi Brancato,[5] Lukman Hakim,[1,2,3] Robert Puers[5] and Dirk De Ridder[4]

[1]Faculty of Medicine, Airlangga University, [2]Department of Urology, Dr Soetomo Hospital, [3]Department of Urology, Airlangga University Hospital, Surabaya, Indonesia, [4]Laboratory of Experimental Urology, Department of Development and Regeneration, KU Leuven, and [5]ESAT-MICAS, KU Leuven, Leuven, Belgium

Abbreviations & Acronyms
A.U. = arbitrary units
PDMS = polydimethylsiloxane
TLA = total linear acceleration

Correspondence: Dirk De Ridder M.D., Ph.D., Department of Urology, UZ Leuven, Herestraat 49, Leuven 3000, Belgium. Email: dirk.deridder@uzleuven.be

Received 19 October 2019; accepted 4 March 2020.

Objectives: To test the hypothesis that an implantable sensing system containing accelerometers can detect small-scale autonomous movements, also termed micromotions, which might be relevant to bladder physiology.

Methods: We developed a 6-mm submucosal implant containing a pressure sensor (MS5637) and a triaxial accelerometer (BMA280). Sensor prototypes were tested by implantation in the bladders of Gottingen minipigs. Repeated awake voiding cystometry was carried out with air-charged catheters in a standard urodynamic set-up as comparators. We identified four phases of voiding similar to cystometry in other animal models based on submucosal pressure. Acceleration signals were separated by frequency characteristics to isolate linear acceleration from the baseline acceleration. The total linear acceleration was calculated by the root mean square of the three measurement axes. Acceleration activity during voiding was investigated to adjacent 1-s windows and was compared with the registered pressure.

Results: We observed a total of 19 consecutive voids in five measurement sessions. A good correlation ($r > 0.75$) was observed between submucosal and catheter pressure in 14 of 19 premicturition traces. The peak-to-peak interval between maximum total linear acceleration was correlated with the interval between submucosal voiding pressure peaks ($r = 0.760$, $P < 0.001$). The total linear acceleration was higher during voiding compared with pre- and postmicturition periods (start of voiding/phase 1).

Conclusions: To the best of our knowledge, this is the first report of bladder wall acceleration, a novel metric that reflects bladder wall movement. Submucosal sensors containing accelerometers can measure bladder pressure and acceleration.

Key words: acceleration, animal study, new devices, physiology, urodynamics techniques.

Introduction

Overactive bladder syndrome is defined as urinary urgency and frequency, with or without urgency urinary incontinence.[1] The current technical assessment of symptoms is carried out through urodynamic assessment of bladder pressure changes. Bladder pressure is a net result of overall bladder activity, abdominal pressure and outlet resistance. Events identified through these methods, such as detrusor overactivity, correlate poorly with urgency symptoms.[2,3]

Localized bladder activity, such as a micromovement in the detrusor, has been observed together with a corresponding change in bladder pressure, but also without any effect on bladder pressure.[4] These micromotions were initially observed visually as autonomous activity in bladder strips and isolated bladder preparations. The role of these micromotions in normal and pathological bladder physiology in large animals and eventually humans could be further elucidated if adequate measurement tools are developed.[5]

Accelerometers implanted intramurally can locally measure motion of an organ part.[6] These acceleration sensors are closed, self-contained systems that do not require an open window with the surrounding environment, unlike pressure sensors. As such, their output is more stable and far less susceptible to changes occurring in the encapsulation materials or the

surrounding tissues. The use of an implantable epicardial accelerometer recorded real-time motion signals for identification of cardiac dysfunction.[6,7] In the urinary tract, multiple accelerometers built into a urethral catheter have been designed for tracking bladder neck position in stress urinary incontinence.[8] Other signals generated by bladder wall cells are electromyographic signals that need to be recorded by specialized electrodes. However, *in vivo* measurement methods are limited by artifacts resulting from mechanical signals.[9]

Standard methods of bladder pressure measurement using catheters are unsuitable for long-term use because of the risk of infection. In current clinical practice, ambulatory urodynamic examination using different catheters are limited to <24 h of observation.[10] Recently, devices for suburothelial implantation were reported for long-term pressure monitoring of the bladder.[11,12] This location prevents direct contact with urine and reduces the risk of encrustation, while preserving sensitivity of the pressure measurement.

Our goal was to design an implantable sensor containing an acceleration sensor in addition to a pressure sensor placed in the submucosa of the bladder wall for long-term measurement of bladder wall activity. In the present study, we describe *in vitro* and *in vivo* testing of the device, and the preliminary analysis of acceleration data in an awake animal model. This model was chosen to measure acceleration in voiding, a physiologically significant movement of a large amplitude. As this is the first study of bladder acceleration, we need to examine the characteristics of acceleration signals produced by the bladder, develop analytical steps and show its relevance to its voiding events.

Methods

Implant design

The implant is based on a flexible circuit board with a circular submucosal portion 6 mm in diameter. This sensing implant contains an accelerometer (BMA 280; Bosch Sensortec GmbH, Reutlingen, Germany), as well as a pressure sensor (MS5637; TE Connectivity, Schaffhausen, Switzerland; Fig. 1). These components were off-the-shelf, commercially available microchips, selected based on small dimensions and low power consumption. The pressure sensor measures $3 \times 3 \times 0.9$ mm^3 and has a built-in analog-to-digital convertor. The average current drain is 150 μA (at 250-Hz sampling rate). It has an I2C interface for digital communication. That is also the case for the accelerometer, which measures $2 \times 2 \times 0.95$ mm^3 and consumes 130 μA while sampling at 2 kHz. The combined sensors were encapsulated with Parylene-C, medical epoxy (EPO-TEK 302-3M; Epoxy Technology Inc., Billerica, MA, USA) and medical grade PDMS (MED-6017; NuSil Technology, Carpinteria, CA, USA), compatible for long-term implantation.[6,13] The deposition of medical polymers on the sensitive silicone membrane strongly affects the pressure-sensing characteristics of the device. For this reason, all pressure sensors were recalibrated after the fabrication process. The sensor system incorporated a microcontroller that is sampling the sensors at their respective frequencies, and provides communication over the universal asynchronous receiver–transmitter protocol. The Microchip Technology PIC12LF1552 controller is selected for its small size. Full details on the fabrication and design of the sensor and supporting unit have been published.[14,15]

Bench testing

We tested the submucosal implantation technique in two explanted porcine bladders. After incision of the seromuscular layer and creation of a submucosal pocket, we inserted the sensor with the pressure transducer oriented toward the lumen and fixed with non-absorbable sutures (3-0 polypropylene). An indwelling 18-Fr Foley transurethral catheter was inserted. Saline filling was carried out manually until a volume of 500 mL was reached. The bladder was allowed to empty through the catheter without additional external pressure.

Experimental animals

All animal experiments were carried out with approval from the institutional Ethical Committee for Animal Research. Long-term implants were carried out on four female Gottingen minipigs 20–24 months-of-age (60–70 kg). The bladder dome was exposed through a lower abdominal incision, the device was submucosally inserted and fixed by non-absorbable sutures at the midline of the bladder dome (or also referred to as apex;[16] Fig. 2). After a post-surgical recovery period of 7 days, the animals were temporarily anesthetized

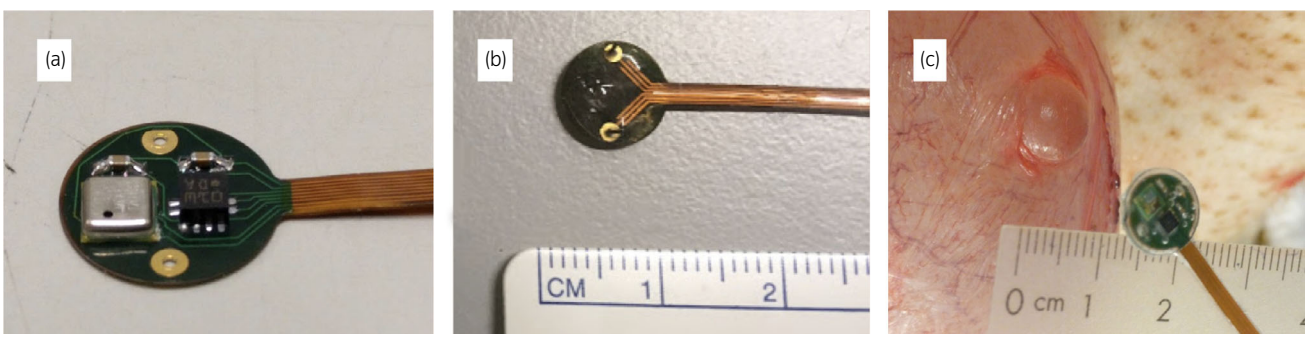

Fig. 1 Implantable pressure and acceleration sensor. (a) Unencapsulated flexible board showing sensors. (b) Posterior aspect of sensor encapsulated by PDMS encapsulated. (c) Implantation procedure by access to submucosa, protrusion of mucosa showing complete separation of serous layer.

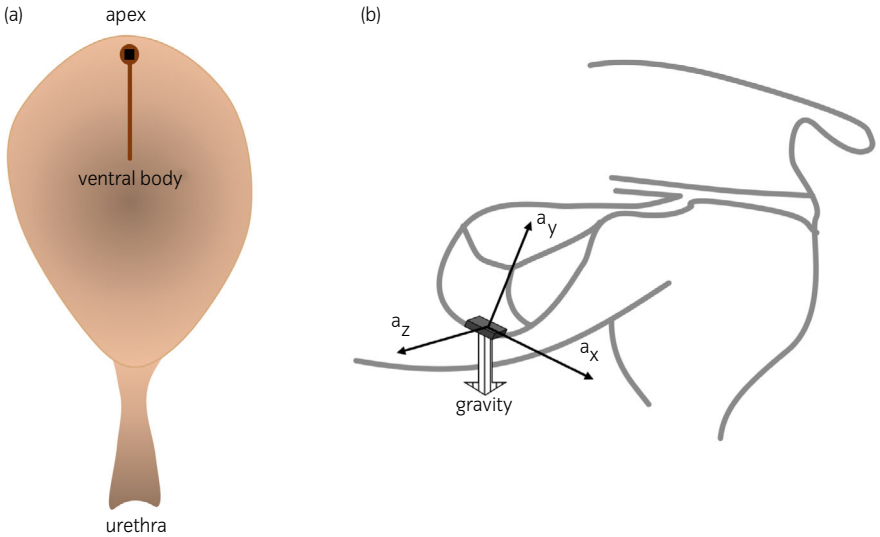

Fig. 2 Location of implantation in detail. (a) Sensor submucosally inserted at the bladder apex as described by Borsdorf *et al.*[16] (b) Anatomical location of sensor and three-dimensional acceleration directions.

with ketamine (15 mg/mL i.m.) and xylazine (2 mg/kg i.m.) for urethral instrumentation. This anesthetic regimen was selected from the minipig literature for the following reasons: (i) sufficient muscle relaxation of the urethral sphincter to allow passage of catheter and instruments; (ii) rapid onset and recovery with sufficient duration of anesthesia; and (iii) most importantly, spontaneous voiding after return of consciousness. In preliminary experiments, minipigs did not void under anesthesia and other regimens did not result in consistent voiding up to 12 h post-recovery.

We inserted a three-way 7-Fr urodynamic catheters (T-DOC-7FDR) connected to a Laborie Aquarius TT urodynamic system (Laborie Medical Technologies Europe, Bristol, UK). We awaited signs of post-anesthetic recovery marked by the animal spontaneously standing. We carried out consecutive filling cystometries by infusion of normal saline at 50 mL/min until at least three consecutive voiding events were observed.

Description of pressure and accelerometer data

Pressure curves during micturition were described with voiding phases adapted to the porcine model described in Figure 3.[17] The start of voiding was identified by the initial increase of pressure until the first pressure peak. The end of voiding was the period from the second pressure peak until return to baseline pressure.

Acceleration is reported as G-forces (g) and processed as outlined in Figure 4. The recorded acceleration signal consisted of high-frequency oscillatory bursts of linear acceleration and a baseline value. This baseline was determined by the orientation of a particular axis relative to gravity. Linear acceleration was obtained by a high-pass filter at 0.15 Hz, whereas the baseline was obtained by low-pass filter at the same cut-off frequency. Change in the baseline value (Δa) is calculated by subtraction of the start value from the end value.

We combined the movement in the three axes to calculate the TLA, which was defined as the root mean square of the three linear acceleration components along the perpendicular

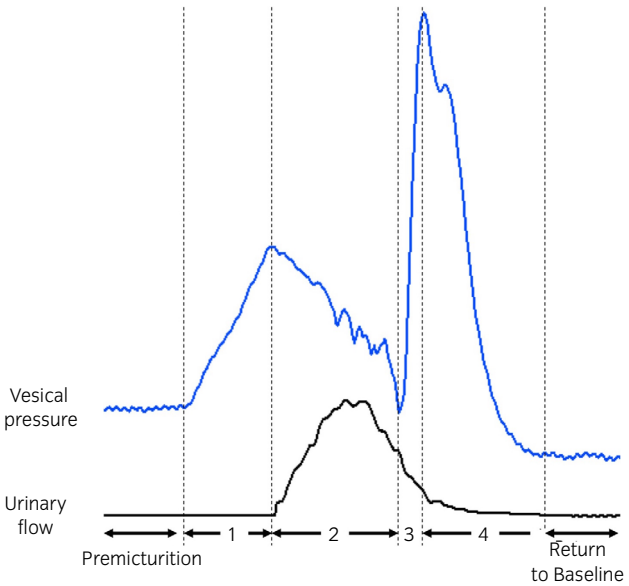

Fig. 3 Phases of porcine micturition (adapted from Andersson *et al.*).[17] Phase 1 – initial increase of intravesical pressure. Phase 2 – flow of urine. Phase 3 – rebound increase in intravesical pressure. Phase 4 – rapid pressure decline to the level before the micturition contraction.

sensitive axes ($\mathrm{TLA} = \sqrt{\hat{a}_x^2 + \hat{a}_y^2 + \hat{a}_z^2}$). To compare differences of linear acceleration between the voiding phases, we calculated the mean TLA from the entirety of each phase. To observe the change in bladder activity at the start and end of voiding, we took 1-s periods immediately before and after voiding periods as comparison.

Statistical analysis

Acceleration values are expressed as the median (interquartile range) unless otherwise specified. The difference between voiding periods was tested by the Wilcoxon matched-pairs signed-rank test. The duration of voiding periods measured was compared by Spearman's correlation. The linear

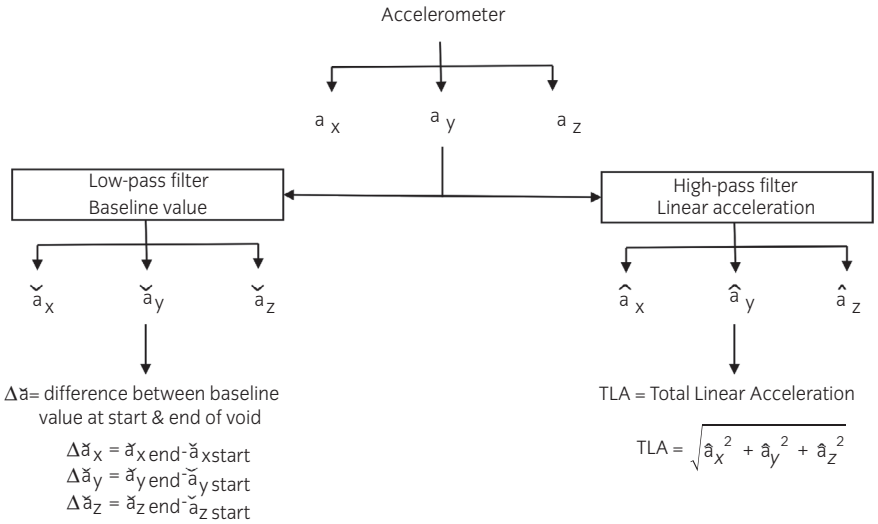

Fig. 4 Overview of data processing. Acceleration was measured in three axes (*x*-, *y*- and *z*-) and subsequently filtered. Low-pass filter isolated low-frequency signals resulting in baseline value. High-pass filter isolated high-frequency signals of linear acceleration, values in three axes were combined by root mean square reported as TLA.

relationship between pressure values measured was evaluated by the Pearson correlation coefficients. A *P*-value of <0.05 was considered indicative of statistical significance. The difference of histological bladder wall thickness was compared by the Mann–Whitney test. Statistical analyses were carried out using Graphpad Prism 7.0 (Graphpad Software, San Diego, CA, USA) and Origin Pro 9 (Originlab Corporation, Northampton, MA, USA).

Results

Bench testing

Data showing three filling cycles of an explanted bladder are shown in Figure 5. The submucosal acceleration increased during active filling and decreased when filling was stopped. In the same period, the bladder pressure showed limited change. Emptying resulted in an increase of both acceleration and pressure. Pressure values by the implanted sensor were correlated with the catheter measurements (Pearson's $r = 0.91$, $P < 0.001$). No mucosal extrusion of the implant was observed after 10 filling and emptying cycles. On intraluminal inspection, there was no difference in the sensor position after repeated emptying compared with the original position.

Animal implants

Surgical implantation of the sensor in minipigs was carried out in four animals. In the first implantation, although no movement data were recorded, we obtained valuable input on material and packaging properties in addition to an *in vivo* test of power and data circuits. All measurements were carried out through a wired connection tunneled to the flank.

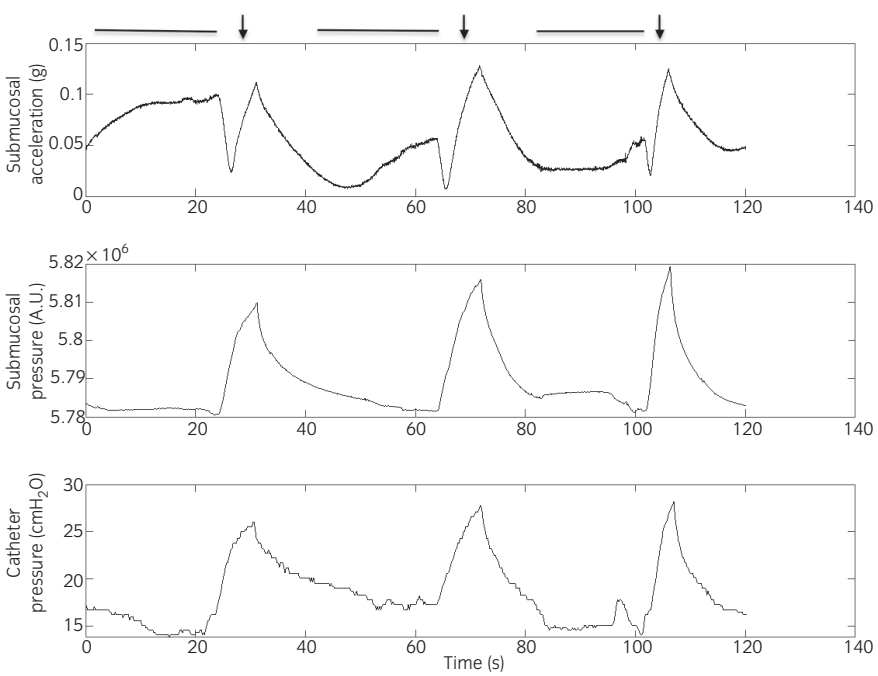

Fig. 5 Pressure and baseline acceleration *in vitro* from isolated porcine bladder. Horizontal lines mark periods of bladder filling, arrows mark emptying. Raw output of submucosal pressure measurement is reported in A.U.

We carried out five sessions of consecutive voiding cystometry with a recording duration of 70 min (32.7 min) per session. There were four voids per session (range 3–5) for a total of 19 voiding events. The bladder filling volume was 664 mL (509.5 mL) at the time of voiding. In this study, we focused on the period surrounding the voiding events where animals were stationary and movement artifacts were limited. Intravesical pressure changes observed with the submucosal device corresponded with the catheter measurements, as shown in Figure 6. The submucosal pressure recording required less time to return to the baseline compared with the catheter measurement. The duration of voiding, measured from initial pressure increase until return to baseline, was 80.9 s (22.2 s) and 93.1 s (44.0 s) for submucosal and catheter measurements, respectively ($P = 0.055$).

Overall, the submucosal pressure values differed from catheter pressure measurement by -10.1 ± 27.1 mbar (mean ± SD). The correlation of values between both measurement methods was 0.29 ($P < 0.0001$). Pressure curves were markedly different after the first voiding peak between submucosal and catheter measurements (Fig. 6a,c). The correlation of measured pressure values are shown in Table 1. The pressure correlation was higher before the first voiding peak ($r = 0.42$–0.98), than after this point ($r = 0.19$–0.91).

Animal implants: Cystometry data and multiple measurements

In two of five measurement sessions, the catheter sensitivity was reduced after the first voiding event (Fig. 6b). Measurements of the first void event had a good correlation ($r = 0.72$–0.98), whereas subsequent voids had a correlation between $r = 0.42$–0.94 (Table 1). Measurement in subsequent weeks did not consistently show lower correlation coefficients. The correlation at the longest implantation period at 4 weeks remained high ($r = 0.77$–0.97).

Animal implants

We divided the voiding into four phases adapted from other animal models, as shown in Figure 3. The acceleration in three axes surrounding a voiding event with the accompanying pressure curve is shown in Figure 7a. The orientation of an accelerometer relative to gravity determines the baseline acceleration value in each axis, therefore the wall orientation reflected in this value is affected by bladder morphology, wall tension and volume. The value of the baseline Δa was higher during voiding compared with the immediate pre- and postmicturition periods (Fig. 7b).

The bladder wall movements also resulted in a linear acceleration. The linear acceleration from the three axes was combined as described. The interval between the maximum TLA correlated with the interval between peaks of submucosal voiding pressure (Spearman's $r = 0.59$, $P = 0.0098$). The average TLA during each voiding period is presented in Figure 7c. During the first voiding phase, the TLA was higher than in the premicturition period (66.0 [36.0] *vs* 26.6 [47.8] $\times 10^{-3}$ g, $P = 0.0095$). The TLA at the end of the voiding (phase 4) and postmicturition were 22.1 (22.2) $\times 10^{-3}$ g and 14.7 (24.1) $\times 10^{-3}$ g ($P = 0.036$), respectively.

Drawbacks

After device implantation, animals did not show signs of distress. Local irritation around the exit wound of the percutaneous wires was observed in one animal at 2 weeks

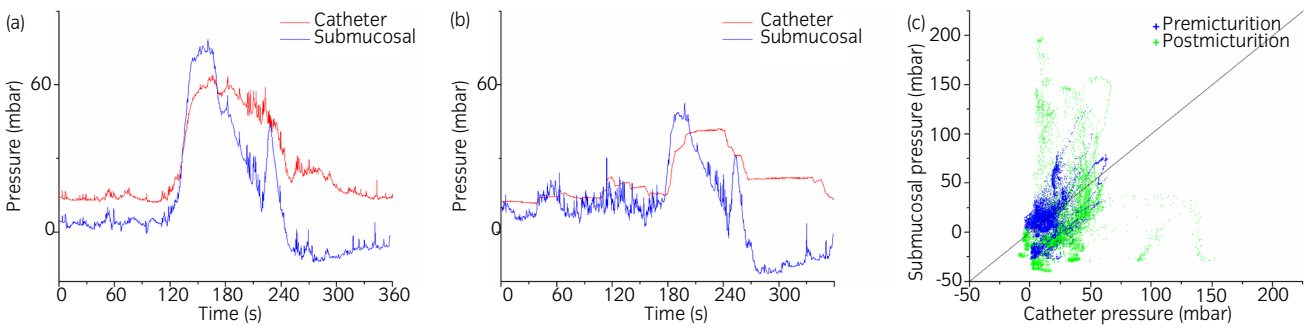

Fig. 6 *In vivo* intravesical pressure measurement. (a,b) Sample recording of submucosal pressure from the (a) first and (b) third consecutive voiding. (c) Scatterplot of catheter compared with submucosal pressure before and after first micturition peak (corresponding to end of phase 1 in Fig. 3).

Table 1 Correlation of pressure value between submucosal sensor and intravesical catheter

Device	Week	Before voiding peak					After voiding peak				
1	1	0.88	0.80	0.89			0.54	0.19	0.56		
	2	0.72	0.46	0.42			0.66	0.30	0.29		
2	1	0.86	0.75	0.86	0.88	0.89	0.76	0.65	0.83	0.79	0.52
	2	0.98	0.94	0.64	0.47		0.91	0.89	0.86	0.53	
	4	0.97	0.77	0.94	0.83		0.30	0.50	0.79	0.62	

Values are Pearson correlation coefficient under assumption of linear relationship between both devices ($P < 0.001$ for all values).

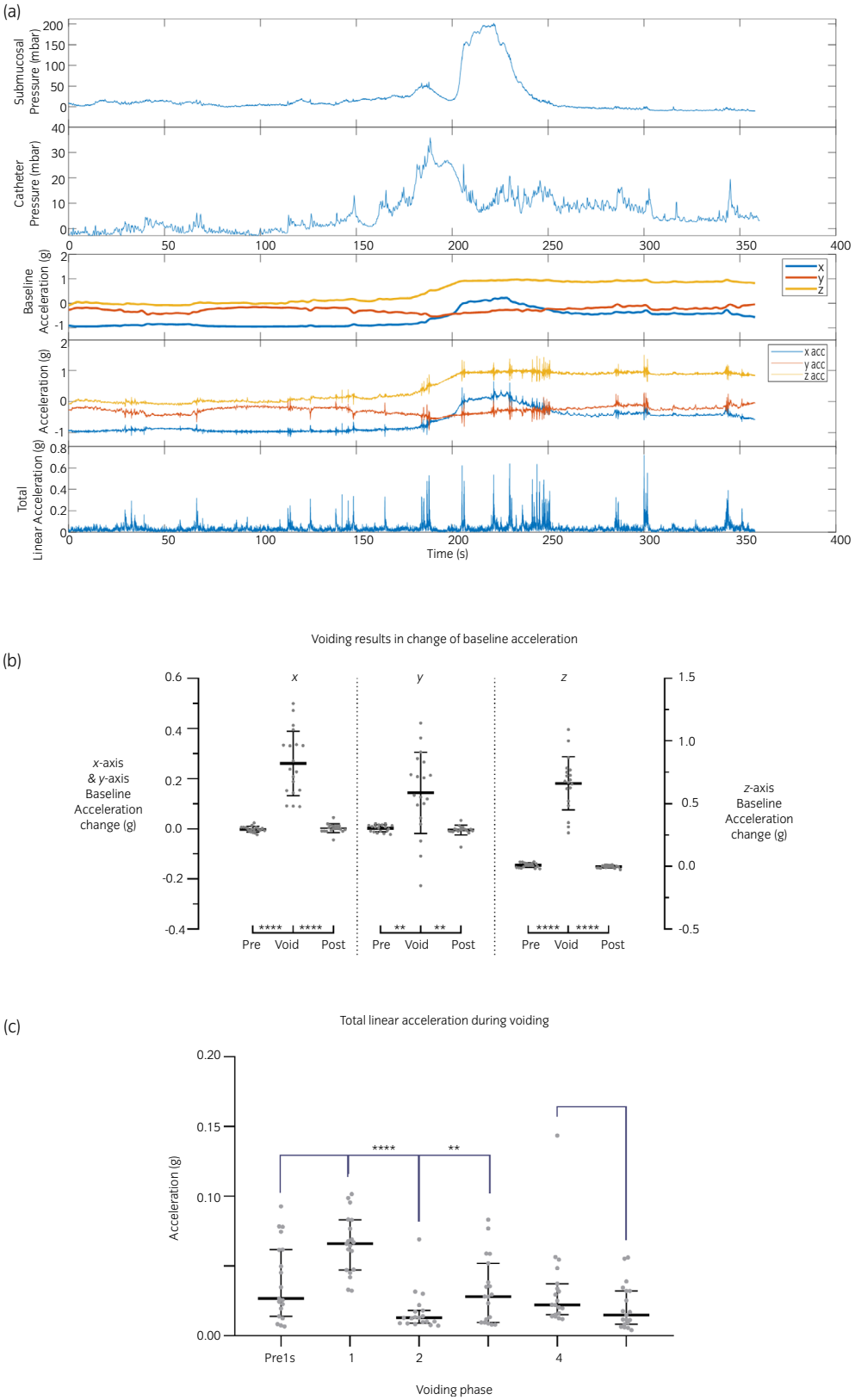

Fig. 7 Bladder pressure and acceleration during voiding. (a) Bladder pressure, tri-axial acceleration, low-frequency signals of gravity component and high-frequency signals of linear acceleration. Total acceleration calculated by root mean square. (b) Change of baseline acceleration during voiding compared with 1-s period pre- and postmicturition. (c) Bladder activity as area under the curve of TLA divided by duration of voiding period. Statistical testing by Wilcoxon matched-pairs signed rank test. *$P < 0.05$, **$P < 0.01$, ***$P < 0.001$, ****$P < 0.0001$.

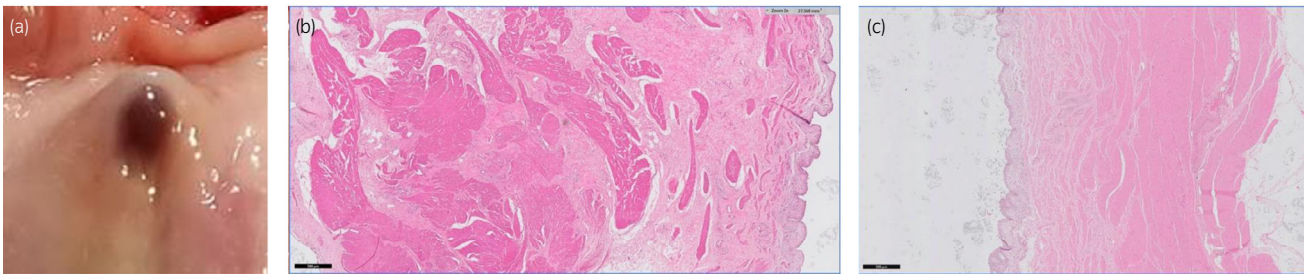

Fig. 8 Tissue reaction after 4 weeks implantation. (a) Intraluminal aspect. (b,c) Histological view of bladder tissue (hematoxylin–eosin) from submucosal implant and control sites (respectively). Thickness of the bladder wall is measured as an average of at least three different sites (magnification: ×2). Bladder wall thickness was 7.16 ± 0.17 mm at implantation site and 5.39 ± 0.29 mm at control locations (P = 0.009, Mann–Whitney test).

post-implantation, leading to explantation. The diffusion of moisture in the packaged sensor system caused the first device to fail after an implantation time of 3 days. Improvement in the packaging technique allowed us to achieve 2 and 4 weeks implantation time in later iterations. On device explantation, all sensors were found *in situ* at the site of implantation. We observed no breakage of the mucosa in all animals. Histological examination after 4 weeks of implantation showed thickening and disruption of the muscle layer where devices were implanted (Fig. 8), but no signs of infection, or severe fibrosis.

Discussion

We report a novel submucosal implant combining pressure with acceleration sensors in the bladder submucosa. The final prototype was functional for more than 4 weeks after initial implantation. Pressure measured with the implant maintained sensitivity over the study period and correlated with standard urodynamic catheter measurement. Measurement of acceleration on the bladder provided a novel measure of activity with a pattern related to voiding.

Use of implants has been previously reported to enable a method for long-term bladder pressure monitoring.[11] Pressure measurement instruments can be placed either within the bladder lumen or in the bladder submucosa. Intraluminal devices might require an opening of the bladder mucosa and carry the risk of calculus formation.[18] Submucosal implantation avoids direct contact with urine, which reduces the risk of encrustation while placing tissue overlying the sensing membrane of the pressure microchip.[11] Another disadvantage of implants is the inability to adjust zero value by simple exposure to atmospheric pressure. Despite these limitations, we observed that the pressure values from the submucosal implant remained within the physiological range during the study period. Additionally, sensitivity to changes in intravesical pressure was maintained with good correlation with catheter values reported up to the final week of measurements.

Previous research into implants was motivated by triggered neuromodulation as a promising application. This emphasizes rapid transmission of changes in bladder pressure over absolute accuracy of pressure measurement.[11] There was a significant correlation between the implanted pressure sensor and the urethral catheter. In one animal, a significant movement artifact was observed as a result of skin irritation, and a lower correlation was observed. There was more variation in pressure during voiding, which might be caused by variable contact of the sensing membrane with the urothelium and changes in transmission of urine pressure. In the measurement of repeated voiding, a lower correlation was observed in subsequent voids compared with the initial voids. In some cases, the decrease in correlation was due to the type of urethral catheter chosen as a comparator in the present study, which showed decreased measurement sensitivity (Fig. 6b). The air-charged catheter was chosen to avoid movement artefacts; however, a drift over long-term measurement has been reported.[19] Additionally, sensing membrane characteristics might become augmented as a result of mucosal contact, and adherent mucus precipitation might play a role. Similar decreases in sensitivity were previously reported in the measurement of consecutive voiding.[20] In the last week, pressure measurements showed a similar range of correlations with the initial measurements. The characteristics of submucosal pressure measurement were consistent with results previously published.[11,21]

We observed voiding pressure in minipigs both before and after sensor implantation.

Before sensor implantation, we carried out cystometry in the same minipigs housed in metabolic cages with uroflowmetry recording (Fig. 3). The voiding pressure traces showed a bimodal curve similar to previous studies in minipigs,[18] therefore we decided to adapt the voiding phases as described by Andersson *et al.*[17]

Using our implantable sensor, we looked at the distribution of the acceleration at the start and end of voiding, as marked by changes in intraluminal pressure. The increase in linear acceleration marked the start and end of voiding. In contrast, the baseline accelerometer value shifted gradually during voiding, which reflects a change in sensor orientation relative to the direction of gravity. This corresponds with results from three-dimensional imaging, where the orientation of bladder surfaces varies at different volumes.[22]

Furthermore, the findings prove that implantable accelerometers can be used to define several phases of the voiding (and filling phase). Measuring linear acceleration at a single point on the bladder wall could yield information about eventual micromotions or segmental bladder wall movements, that might play a role in afferent signaling and the generation of the urgency sensation. However, this can only be retrieved in a comparative or differential method, to avoid interference with

overall body movements. To compare acceleration measures from different locations, a device with multiple sensors are in development. Therefore, in future projects, we will focus on a multipoint device with distributed accelerometers over the bladder wall that allows us to compare acceleration recorded simultaneously from different parts.

There were several limitations of our device. First, this sensor required open surgical access to the bladder for implantation. Some prototypes proved to be too vulnerable for use in minipigs. Connections and wireless transmission units deserve further attention in future work. At this moment, we mainly focused on the voiding phase (because of the minimal movements of the animals during this event). Studying the filling phase using accelerometer data will generate interesting data. In these experiments, pharmacological challenges (e.g. anticholinergics, intravesical irritants) will be used to modulate the filling phase.

The development of a tailored microchip design might succeed in smaller devices with wireless communication, allowing future endoscopic insertion. Second, only a limited number of devices were implanted to minimize the use of animals.

In conclusion, an implantable sensor for pressure and acceleration measurement in the bladder wall provides novel information on local and general bladder behavior. Submucosal pressure correlated with standard intraluminal methods and performed better in long duration. To our knowledge, this is the first description of acceleration signals from the bladder. Accelerometer signals capture bladder wall motion and orientation, which characterized voiding from non-voiding periods, as well as the different phases of voiding. A network of multiple accelerometers has the potential for a longitudinal study of the bladder *in situ*, leading to a better understanding of bladder behavior.

Acknowledgments

This research received funding from the European Research Council (ERC-2013-AG) and MicroThalys, grant agreement No. 340931. MAS received support from the Indonesian Endowment Fund for Education (LPDP).

Conflict of interest

None declared.

References

1 Haylen BT, de Ridder D, Freeman RM *et al*. An International Urogynecological Association (IUGA)/International Continence Society (ICS) joint report on the terminology for female pelvic floor dysfunction. *Neurourol. Urodyn.* 2010; **29**: 4–20.

2 Leitner L, Walter M, Sammer U, Knüpfer SC, Mehnert U, Kessler TM. Urodynamic investigation: a valid tool to define normal lower urinary tract function? *PLoS One* 2016; **11**: e0163847.

3 Hashim H, Abrams P. Is the bladder a reliable witness for predicting detrusor overactivity? *J. Urol.* 2006; **175**: 191–4.

4 Drake MJ, Kanai A, Bijos DA *et al*. The potential role of unregulated autonomous bladder micromotions in urinary storage and voiding dysfunction; overactive bladder and detrusor underactivity. *BJU Int.* 2017; **119**: 22–9.

5 Drake MJ, Fry CH, Hashitani H *et al*. What are the origins and relevance of spontaneous bladder contractions? ICI-RS 2017. *Neurourol. Urodyn.* 2018; **37**: S13–9.

6 Brancato L, Weydts T, Oosterlinck W, Herijgers P, Puers R. Packaging of implantable accelerometers to monitor epicardial and endocardial wall motion. *Biomed. Microdevices* 2017; **19**: 52.

7 Grymyr O-JHN, Beitnes JO, Eidet J *et al*. Detection of intraoperative myocardial dysfunction by accelerometer during aortic valve replacement. *Interact. Cardiovasc. Thorac. Surg.* 2016; **24**: ivw326.

8 Sun H, Fu G, Xie H. A MEMS accelerometer-based real-time motion-sensing module for urological diagnosis and treatment. *J. Med. Eng. Technol.* 2013; **37**: 127–34.

9 Hammad FT. Electrical propagation in the renal pelvis, ureter and bladder. *Acta Physiol.* 2015; **213**: 371–83.

10 Rademakers KLJ, van Koeveringe GA, Oelke M. Detrusor underactivity in men with lower urinary tract symptoms/benign prostatic obstruction. *Curr. Opin. Urol.* 2016; **26**: 3–10.

11 Majerus SJA, Fletter PC, Ferry EK, Zhu H, Gustafson KJ, Damaser MS. Suburothelial bladder contraction detection with implanted pressure sensor. *PLoS One* 2017; **12**: e0168375.

12 Melgaard J, Struijk JJ, Rijkhoff NJM. Minimizing a wireless passive LC-tank sensor to monitor bladder pressure: a simulation study. *J. Med. Biol. Eng.* 2017; **37**: 800–9.

13 Brancato L, Weydts T, De Clercq H, Dimiaux T, Herijgers P, Puers R. Biocompatible packaging and testing of an endocardial accelerometer for heart wall motion analysis. *Procedia Eng.* 2015; **120**: 840–4.

14 Weydts T, Deruyver Y, Brancato L *et al*. 348 Developing a long-term implantable system to accurately measure real-time bladder wall movements: a feasibility study in the rat. *Eur. Urol. Suppl.* 2016; **15**: e348.

15 Brancato L, Weydts T, Soebadi MA, De Ridder D, Puers R. Submucosal exploration of EMG and physiological parameters in the bladder wall. *Proceedings* 2017; **1**: 605.

16 Borsdorf M, Tomalka A, Stutzig N, Morales-Orcajo E, Böl M, Siebert T. Locational and directional dependencies of smooth muscle properties in pig urinary bladder. *Front. Physiol.* 2019; **10**: 1–12.

17 Andersson K-E, Soler R, Füllhase C. Rodent models for urodynamic investigation. *Neurourol. Urodyn.* 2011; **30**: 636–46. https://doi.org/10.1002/nau.211081

18 Huppertz ND, Kirschner-Hermanns R, Tolba RH, Grosse JO. Telemetric monitoring of bladder function in female Göttingen minipigs. *BJU Int.* 2015; **116**: 823–32.

19 Couri BM, Bitzos S, Bhardwaj D, Lockhart E, Yue A, Goping I. Performance analysis of the T-DOC® air-charged catheters: an alternate technology for urodynamics. *Neurourol. Urodyn.* 2018; **37**: 619–25.

20 Soebadi MA, Bakula M, Hakim L, Puers R, De Ridder D. Wireless intravesical device for real-time bladder pressure measurement: study of consecutive voiding in awake minipigs. *PLoS One* 2019; **14**: e0225821.

21 Basu AS, Majerus S, Ferry E, Makovey I, Zhu H, Damaser MS. Is submucosal bladder pressure monitoring feasible? *Proc. Inst. Mech. Eng. Part H. J. Eng. Med.* 2019; **233**: 100–13.

22 Lotz HT, van Herk M, Betgen A, Pos F, Lebesque JV, Remeijer P. Reproducibility of the bladder shape and bladder shape changes during filling. *Med. Phys.* 2005; **32**: 2590–7.